D-D Nuclear Fusion Using Different Size Pyroelectric Crystals

A. M. Kovanen, D. J. Gillich, T. Z. Fullem, and Y. Danon

Abstract– **Theory predicts electrons play a detrimental role in creating the conditions for D-D fusion in pyroelectric crystal accelerators. Three different pyroelectric crystal sizes were paired in six different configurations to determine if experimental results agree with theory. An experimental configuration using a 30 mm diameter tip crystal opposite a 20 mm diameter target crystal yielded better neutron results than a 20 mm diameter tip crystal versus a 30 mm diameter target crystal as predicted by theory. Two 20 mm diameter by 20 mm thick lithium tantalate crystals yielded ~1 × 10^4 neutrons per thermal cycle.**

I. Introduction

Pyroelectric crystals exhibit a nonzero spontaneous polarization due to the dipole moments of the crystal unit cells [1] and can be cut such that the dipole moments are perpendicular to the flat surfaces, known as the $+z$ and $-z$ faces. As a pyroelectric crystal experiences a temperature change, the dipole moments either become more or less aligned with the z faces resulting in the spontaneous polarization either increasing or decreasing. This change in polarization causes charge to build on the z faces. The amount of charge induced on a z face, φ, is given by [2]:

$$\varphi = \gamma A_{cr} \Delta T \tag{1}$$

where γ is the pyroelectric coefficient of the crystal, A_{cr} is the surface area of one of the crystal's z faces, and ΔT is the change in temperature. Since little if any charge migrates through the crystal, pyroelectric crystals can be modeled as parallel plate capacitors with a capacitance, C_{cr}, given by:

$$C_{cr} = \varepsilon_{cr} \varepsilon_0 A_{cr} / t_{cr} \tag{2}$$

where ε_{cr} is the relative permittivity of the crystal, ε_0 is the permittivity of free space, and t_{cr} is the thickness of the crystal. For a two-crystal configuration in which opposite polarity z faces oppose each other, the accelerating potential, V, is given by:

$$V = 2\varphi / C_{cr} \tag{3}$$

For the two-crystal system shown in Fig. 1 using cylindrical lithium tantalate ($LiTaO_3$) crystals ($\gamma = 190\ \mu C/m^2/K$, $\varepsilon_{cr} = 46$) [3] with a diameter of 30 mm and thickness of 10 mm, theory predicts the charge induced on each crystal face after undergoing a 100 K temperature change is 13.4 μC with an accelerating potential of 933 kV between the crystals. However, 200 kV accelerating potentials for such a system are more typical, likely due to the effects of charge migration and parasitic capacitance [4]. The theoretical limit of neutron production for the system described above with a 200 kV accelerating potential is about 2 × 10^7 neutrons per cooling cycle [5]. This calculation assumes the electric field near the field-enhancing tip is sufficiently high such that each induced positive charge results in the ionization and dissociation of a D_2 gas molecule into two D^+ ions and that every D^+ ion accelerates into a deuterated polyethylene (CD_2) target and fuses to a deuterium atom. This calculation also takes into account the fact that each D-D fusion event only has about a 50% chance of producing a neutron.

Currently, neutron production from D-D fusion using pyroelectric crystals is orders of magnitude below the theoretical limit. Typical neutron yields are 10^3 neutrons per thermal cycle with some isolated events reaching 10^4 to 10^5 neutrons per thermal cycle [5]-[7]. A possible reason for low neutron production may be due to the effects of electrons accelerated from the target crystal to the tip crystal. These electrons could neutralize some of the tip crystal's positive charge, hampering the mechanisms of neutron production already explained. The electrons could also provide a path to ground the z face of the tip crystal which would completely stop neutron production. This research presents findings on attempts to reduce the negative effects electrons have on neutron production by using different size pyroelectric crystals.

II. Experimental Methods

$LiTaO_3$ crystals of three different sizes were used in this research. Table I lists the pertinent information of each crystal as well as the acceleration potential and induced charge on the z face relative to a 20 mm diameter, 10 mm thick crystal.

TABLE I. CRYSTAL DATA

Name	Diameter (mm)	Thickness (mm)	Relative Charge	Relative Potential
Short (S)	20	10	1	1
Wide (W)	30	10	2.25	1
Long (L)	20	20	1	2

Manuscript received November 13, 2009. This work was supported by the U. S. Department of Homeland Security under cooperative agreement number 2007-DN-077-ER0003.

The authors are with the Department of Mechanical, Aerospace and Nuclear Engineering, Rensselaer Polytechnic Institute, Troy, NY.

A. M. Kovanen, D. J. Gillich are also with the Department of Physics, United States Military Academy, West Point, NY.

(e-mail: danony@rpi.edu).

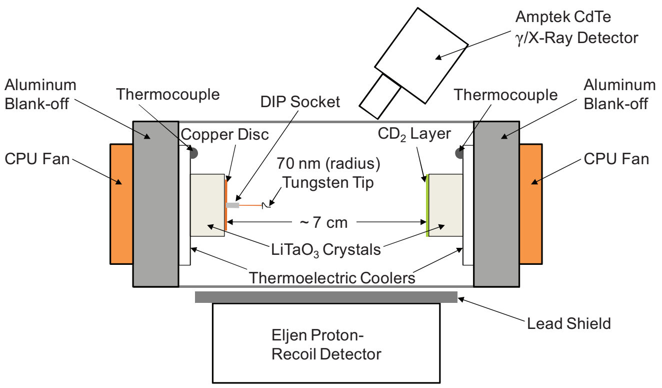

Fig. 1. Experimental setup. There was 7 cm between crystals when both crystals were 10 mm thick.

The *-z* face of a $LiTaO_3$ crystal was mounted with conductive epoxy to a piece of copper tape that covered one side of a thermoelectric cooler (TEC). A section of copper tape extended off the TEC in order to ground the *-z* face to the vacuum chamber. Attached to the *+z* face with conductive epoxy (except for one trial during which JB Weld epoxy was used) was a copper disc with a thickness of approximately 0.5 mm and a diameter approximately 4 mm less than the diameter of the crystal upon which it was mounted (e.g. 26 mm diameter copper disc on a 30 mm diameter crystal). In all configurations except one, a dual inline package (DIP) socket was soldered to the center of the copper disc to facilitate the easy changing of tips. All tips used were 70 nm radius tungsten tips except for a single experiment that used a 100 nm radius tungsten tip. After removing the excess copper tape around the base of the crystal on the TEC surface, a bead of insulating lacquer was applied to the base of the crystal and part of the copper tape to prevent discharges coming from the *+z* face of the crystal.

The tip assembly was secured to a 4.5 in Conflat (CF) aluminum blank-off with conductive epoxy. The target assembly was the same as the tip assembly (not considering crystal size) except the *+z* face of the target crystal was mounted to the heater while the *-z* face was covered in deuterated polyethylene. When using two 10 mm thick crystals, the crystals were approximately 7 cm apart once the blank-offs were secured to the vacuum chamber.

Temperature measurement was accomplished with a type T thermocouple mounted to both TECs with JB Weld. The JB Weld surrounding the thermocouple was coated with insulating lacquer. The deuterium gas pressure during experiments ranged from 3 mtorr to 35 mtorr. Typically, the crystals were heated from 30 °C to 130 °C over 5 minutes, remained at 130 °C for 5 minutes, and then cooled to approximately 40 °C over 6 minutes although different temperature profiles were also used. Temperature feedback and control was provided by two independent thermoelectric module controllers. In addition to the computer fans mounted on the air side of the aluminum blank-offs, two 10 inch household fans blew air onto the aluminum flanges for additional cooling.

Detection equipment consisted of a cadmium telluride (CdTe) γ/x-ray detector and an NE-213 liquid scintillator proton-recoil detector. The x-ray detector was used to measure the energies and production rate of Bremsstrahlung x-rays. The maximum x-ray energy served as an indicator of D^+ energy. The proton-recoil detector along with pulse fall time analysis software was used to detect neutrons.

III. RESULTS

Fig. 2 shows the total neutrons emitted for each experimental configuration while Fig. 3 displays the x-ray spectrum for each configuration. Table II presents the salient data from Fig. 2 and Fig. 3 in tabular form. The optimum deuterium gas pressure for the two highest neutron-producing configurations was between 30 and 35 mtorr. The best neutron-producing trials for the other configurations occurred with deuterium gas pressures between 10 and 20 mtorr.

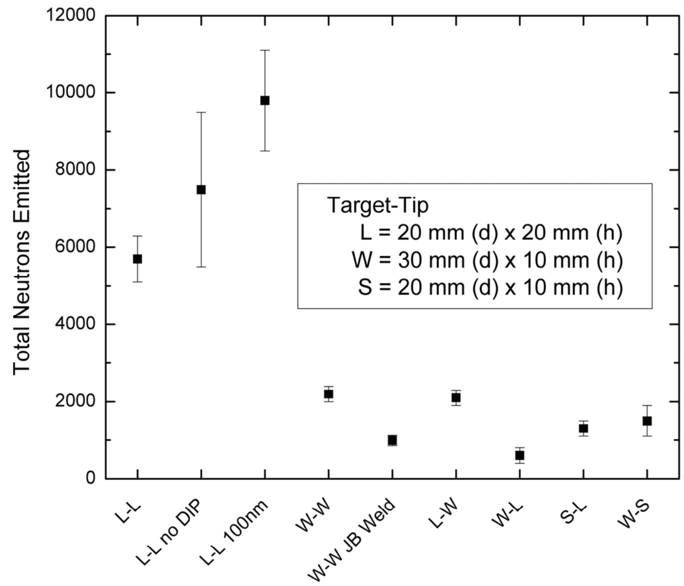

Fig. 2. Total neutrons emitted over 5 minutes after subtracting background and accounting for an absolute detection efficiency of (4.2 ± 0.3) %. Each data point represents the weighted average of three trials weighted by the statistical error with the uncertainties representing the weighted standard deviation of the counts and background counting statistics [8].

The long target-wide tip configuration produced more neutrons (about 3.3 times more) than the wide target-long tip configuration, lending support to the idea that electrons negatively affect the mechanisms of neutron production. If the long target-wide tip configuration only produced 2.25 times as many neutrons as the wide target-long tip configuration, then the difference could be attributed to the 2.25 times greater induced charge on the tip crystal due to it having a *z* face surface area 2.25 times that of the target crystal. However, the multiple being over 2.25 supports the idea that electrons being accelerated away from the target crystal toward the tip crystal have a detrimental effect on neutron production. Although the exact mechanism of how electrons degrade neutron production is unknown, electrons neutralizing positive charge on the tip crystal as well as providing a path to ground the tip crystal likely play a role in reduced neutron production.

The configurations using a long crystal for both the target and the tip produced significantly more neutrons than all other configurations. Although the increased x-ray endpoint energies of the dual long crystal configurations appears to be the obvious explanation for their higher neutron production, it should be noted that the dual long crystal configuration with the 100 nm radius tip produced 175% more neutrons than the standard dual long crystal configuration despite having a 35% lower x-ray endpoint energy. The standard dual wide crystal configuration, which theory predicts should have produced 2.25 times more neutrons than the dual long crystal configurations, only produced one half to one fifth the neutrons as the dual long crystal configurations despite having a similar x-ray endpoint energy.

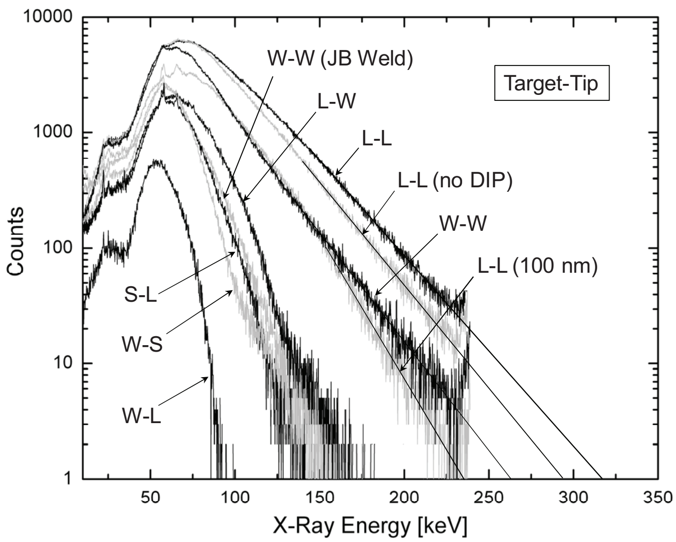

Fig. 3. X-ray spectrum for each experimental configuration. The lines overlaying the last four spectra are used to extrapolate their endpoint energies [8].

TABLE II. X-RAY AND NEUTRON DATA [8]

Configuration (Target-Tip)	X-Ray Endpoint Energy (keV)	Total Neutrons Emitted
Long-Long	318 ± 30	5700 ± 600
Long-Long, no DIP socket	295 ± 28	7500 ± 2000
Long-Long, 100 nm radius tip	236 ± 22	9800 ± 1300
Wide-Wide	264 ± 25	2200 ± 200
Wide-Wide, JB Weld at copper disc/crystal interface	155 ± 15	990 ± 130
Long-Wide	161 ± 10	2100 ± 200
Wide-Long	92 ± 7	610 ± 200
Short-Long	139 ± 13	1300 ± 200
Wide-Short	150 ± 14	1500 ± 200

Inspection of x-ray multichannel scaler (MCS) plots reveals a possible reason why the configurations using wide crystals produced fewer neutrons than the dual long crystal configurations. It can be seen in Fig. 4 that the dual long crystal configurations produced x-rays over a longer period of time as compared to the dual wide crystal configuration. X-ray count rates suddenly dropping or ceasing altogether as shown in Fig. 4 (d) are believed to be caused by electrical arcing between the tip crystal and the vacuum chamber. If true, these so-called discharges would remove most if not all charge from the z face of a crystal and end neutron production. The closest grounding point for a long crystal was the vacuum chamber wall, 21 mm from the edge of the z face. The closest grounding point for a wide crystal was either the wall of the vacuum chamber or the CF blank-off onto which the crystal assembly was mounted, both 16 mm away. The wide crystal being 5 mm closer to a grounding point than the long crystal coupled with the greater number of discharges experienced by the dual wide crystal configuration provides compelling evidence electrons have a negative effect on neutron production.

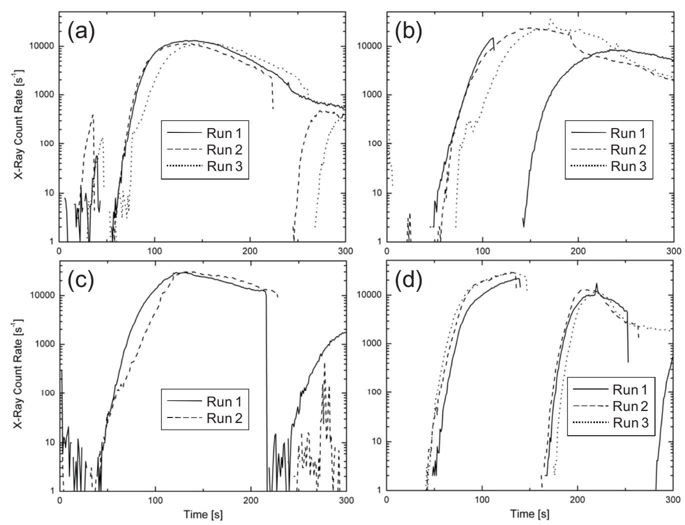

Fig. 4. X-ray MCS plots for (a) dual long crystal configuration with 100 nm tip, (b) dual long crystal configuration with tip soldered to copper disc, (c) standard dual long crystal configuration, and (d) standard dual wide crystal configuration. Plots (a), (b), and (d) show data from three thermal cycles while plot (c) shows data from two thermal cycles [8].

IV. CONCLUSIONS

Experimental evidence supports the theory electrons are detrimental to neutron production in a pyroelectric crystal D-D fusion device. A long target-wide tip configuration produced 3.3 times as many neutrons as a wide target-long tip configuration – greater than the 2.25 multiple expected if electrons did not affect neutron production. The dual wide crystal configuration, which had a grounding point 5 mm closer than the dual long crystal configurations, discharged more than the dual long crystal configurations, an observation not expected if electrons did not affect the system. The dual long crystal configurations produced up to 10^4 neutrons per thermal cycle. The management of electrons should be considered in order to increase neutron production from future pyroelectric crystal D-D fusion devices.

DISCLAIMER

The views expressed herein are those of the authors and do not reflect the position of the United States Military Academy, the Department of the Army, or the Department of Defense.

REFERENCES

[1] S. B. Lang, "Pyroelectricity: from ancient curiosity to modern imaging tool," *Phys. Today*, pp. 31-36, Aug., 2005.

[2] J. A. Geuther, Y. Danon, "High-energy x-ray production with pyroelectric crystals," *J. Appl. Phys.*, vol. 97, 104916, 2005.

[3] S.B. Lang, *Sourcebook of Pyroelectricity*. New York: Gordon and Breach, 1974.

[4] A. M. Kovanen, Y. Danon, D. J. Gillich, "X-ray production using stacked pyroelectric crystals," *ANS Trans*., vol. 98, pp. 406-407, 2008.

[5] D. J. Gillich, "Particle acceleration with pyroelectric crystals," Ph.D. dissertation, Rensselaer Polytechnic Institute, Troy, NY, 2009.

[6] J. A. Geuther, Y. Danon, "Enhanced neutron production from pyroelectric fusion," *Appl. Phys. Lett.,* vol. 90, 174103, 2007.

[7] V. Tang, et al., "Neutron production from feedback controlled thermal cycling of a pyroelectric crystal," *Rev. Sci. Instrum*., vol. 78, Issue 12, 2007.

[8] A. M. Kovanen, "Experiments with D-D fusion from pyroelectric crystal accelerators," M.S. thesis, Rensselaer Polytechnic Institute, Troy, NY, 2009.